

Snap, Crackle, and Pop: Theracoustic Cavitation

Michael D. Gray

Address:

Biomedical Ultrasonics,
Biotherapy and Biopharmaceuticals
Laboratory (BUBBL)
Institute of Biomedical Engineering
University of Oxford
Oxford OX3 7DQ
United Kingdom

Email:

michael.gray@eng.ox.ac.uk

Eleanor P. Stride

Address:

Biomedical Ultrasonics,
Biotherapy and Biopharmaceuticals
Laboratory (BUBBL)
Institute of Biomedical Engineering
University of Oxford
Oxford OX3 7DQ
United Kingdom

Email:

eleanor.stride@eng.ox.ac.uk

Constantin-C. Coussios

Address:

Biomedical Ultrasonics,
Biotherapy and Biopharmaceuticals
Laboratory (BUBBL)
Institute of Biomedical Engineering
University of Oxford
Oxford OX3 7DQ
United Kingdom

Email:

constantin.coussios@eng.ox.ac.uk

Emerging techniques for making, mapping, and using acoustically driven bubbles within the body enable a broad range of innovative therapeutic applications.

Introduction

The screams from a football stadium full of people barely produce enough sound energy to boil an egg (Dowling and Ffowcs Williams, 1983). This benign view of acoustics changes dramatically in the realm of focused ultrasound where biological tissue can be brought to a boil in mere milliseconds (ter Haar and Coussios, 2007). Although the millimeter-length scales over which these effects can act may seem “surgical,” therapeutic ultrasound (0.5-3.0 MHz) is actually somewhat of a blunt instrument compared with drug molecules (<0.0002 mm) and the cells (<0.1 mm) that they are intended to treat.

Is therapeutic acoustics necessarily that limiting? Not quite. Another key phenomenon, acoustic cavitation, has the potential to enable subwavelength therapy. Defined as the linear or nonlinear oscillation of a gas or vapor cavity (or “bubble”) under the effect of an acoustic field, cavitation can enable preferential absorption of acoustic energy and highly efficient momentum transfer over length scales dictated not only by the ultrasound wavelength but also by the typically micron-sized diameter of therapeutic bubbles (Coussios and Roy, 2008). Under acoustic excitation, such bubbles act as “energy transformers,” facilitating conversion of the incident field’s longitudinal wave energy into locally enhanced heat and fluid motion. The broad range of thermal, mechanical, and biochemical effects (“theracoustics”) resulting from ultrasound-driven bubbles can enable successful drug delivery to the interior of cells, across the skin, or to otherwise inaccessible tumors; noninvasive surgery to destroy, remove, or debulk tissue without incision; and pharmacological or biophysical modulation of the brain and nervous system to treat diseases such as Parkinson’s or Alzheimer’s.

Where do these bubbles come from in the human body? Given that nucleating (forming) a bubble within a pure liquid requires prohibitively high and potentially unsafe acoustic pressures (10-100 atmospheres in the low-megahertz frequency range), cavitation has traditionally been facilitated by injection of micron-sized bubbles into the bloodstream. However, the currently evolving generation of therapeutic applications requires the development of biocompatible submicron cavitation nucleation agents that are of comparable size to both the biological barriers they need to cross and the size of the drugs alongside which they frequently travel. Furthermore, the harnessing and safe application of the bioeffects brought about by ultrasonically driven bubbles requires the development of new techniques capable of localizing and tracking cavitation in real time at depth within the human body. And thus begins our journey on making, mapping, and using bubbles for “theracoustic” cavitation.

Making Bubbles

An ultrasound field of sufficient intensity can produce bubbles through either mechanical or thermal mechanisms or a combination of the two. However, the energy that is theoretically required to produce an empty cavity in pure water is significantly higher than that needed to generate bubbles using ultrasound in practice. This discrepancy has been explained by the presence of discontinuities, or nuclei, that provide preexisting surfaces from which bubbles can evolve. The exact nature of these nuclei in biological tissues is still disputed, but both microscopic crevices on the surfaces of tissue structures and submicron surfactant-stabilized gas bubbles have been identified as likely candidates (Fox and Hertzfeld, 1954; Atchley and Prosperetti, 1989).

The energy required to produce cavitation from these so-called endogenous nuclei is still comparatively large, and so, for safety reasons, it is highly desirable to be able to induce reproducible cavitation activity in the body using ultrasound frequencies and amplitudes that are unlikely to cause significant tissue damage. Multiple types of synthetic or exogenous nuclei have been explored to this end. To date, the majority of studies have employed coated gas microbubbles widely used as contrast agents for diagnostic imaging (see article in *Acoustics Today* by Matula and Chen, 2013). A primary disadvantage of microbubbles is that their size (1-5 μm) prevents their passing out of blood vessels (extravasating) into the surrounding tissue. As a consequence, cavitation is restricted to the blood stream. The bubbles are also relatively unstable, having a half-life of about 2 minutes once injected.

There has consequently been considerable research into alternative nuclei. These include solid nanoparticles with hydrophobic cavities that can act as artificial crevices (Rapoport et al., 2007; Kwan et al., 2015). Such particles have much longer circulation times (tens of minutes) and are small enough to diffuse out of the bloodstream into the surrounding tissue. Nanoscale droplets of volatile liquids, such as perfluorocarbons, have also been investigated as cavitation nuclei (see *Acoustics Today* article by Burgess and Porter, 2015). These are similarly small enough to circulate in the bloodstream for tens of minutes and to extravasate. On exposure to ultrasound, the liquid droplet is vaporized to form a microbubble. A further advantage of artificial cavitation nuclei is that they can be used as a means of encapsulating therapeutic material to provide spatially targeted delivery. This can significantly reduce the risk of harmful side effects from highly toxic chemotherapy drugs.

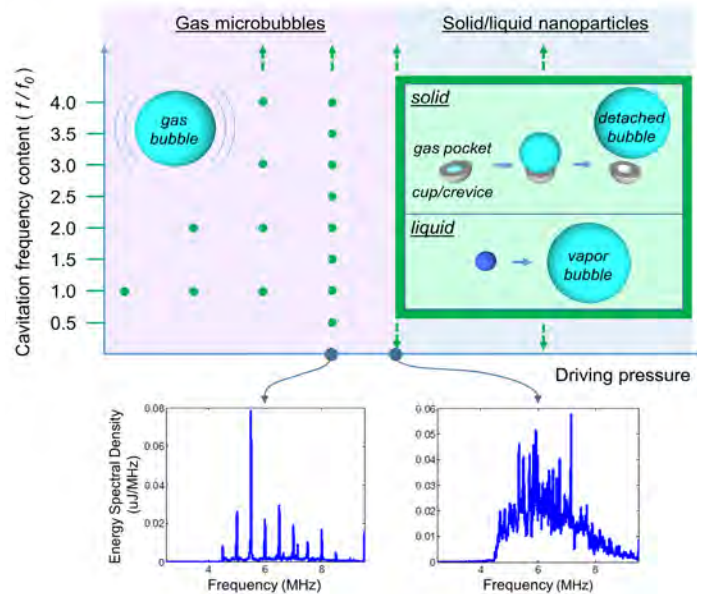


Figure 1. Illustrations of bubble emission behavior as a function of driving pressure. At moderate pressures, harmonics (integer multiples of the driving frequency [f_0]) are produced, followed by fractional harmonics at higher pressures and eventually broadband noise (dashed lines indicate that the frequency range extends beyond the scale shown). Microbubbles (top left) will generate acoustic emissions even at very low pressures, whereas solid and liquid nuclei (top right) require significant energy input to activate them and so typically produce broadband noise. The representative frequency spectra showing harmonic (bottom left) and broadband (bottom right) components were generated from cavitation measurements with $f_0 = 0.5$ MHz.

Cavitation agents also have an advantage over many other drug delivery devices because their acoustic emissions can be detected from outside the body, enabling both their location and dynamic behavior to be tracked. Even at relatively low-pressure amplitudes such as those used in routine diagnostic ultrasound, microbubbles respond in a highly nonlinear fashion and hence their emissions contain harmonics of the driving frequency (Arvanitis et al., 2011). As the pressure increases so does the range of frequencies in the emission spectrum, which will include fractional harmonics and eventually broadband noise (Figure 1). More intense activity, which is normally associated with more significant biological effects, will produce broadband noise. Liquid and solid cavitation nuclei require activation pressures that are above the threshold for violent (inertial) bubble collapse and thus these agents always produce broadband emissions.

Mapping Bubbles

In both preclinical in vivo and clinical studies, a broad spectrum of bubble-mediated therapeutic effects has been demonstrated, ranging from the mild (drug release and intracellular delivery, site-specific brain stimulation) to the malevolent (volumetric tissue destruction). This sizable

range of possible effects and the typical clinical requirement for only a specific subset of these at any one instance underscores the need for careful monitoring during treatment. Despite the myriad bubble behaviors and resulting bioeffects, very few are noninvasively detectible in vivo. For example, light generation during inertial cavitation (sonoluminescence) produced under controlled laboratory conditions may be detectible one meter away, but in soft tissue, both the relatively weak light production and its rapid absorption renders in vivo measurement effectively impossible. Magnetic resonance (MR) techniques, known for generating three-dimensional anatomic images, may also be used to measure temperature elevation, with clinically achievable resolution on the order of 1°C, 1 s, and 1 mm (Rieke and Pauly, 2008). However, because these techniques are generally agnostic to the cause(s) of heating, they cannot mechanistically identify bubble contributions to temperature elevation nor can they generally indicate nonthermal actions of bubble activity. On the basis of high-resolution availability of bubble-specific response cues, active and passive ultrasonic methods appear best suited for noninvasive clinical monitoring.

Active Ultrasound

The enhanced acoustic-scattering strength of a bubble excited near resonance (Ainslie and Leighton, 2011) is exploitable with diagnostic systems that emit and receive ultrasound pulses; bubbles can be identified as regions with an elevated backscatter intensity relative the low-contrast scattering that is characteristic of soft tissues and biological liquids. Intravenous introduction of microbubbles may therefore substantially improve the diagnostic visibility of blood vessels (where microbubbles are typically confined) by increasing both echo amplitude and bandwidth (Stride and Coussios, 2010). Spatial resolution approaching 10 μm may be clinically feasible with “super-resolution” methods employing microbubbles exposed to a high-frame rate sequence of low-amplitude sound exposures (Couture et al., 2018), yielding in vivo microvascular images with a level of detail that was previously unthinkable with diagnostic ultrasound.

Active ultrasound transmissions temporally interleaved with therapeutic ultrasound pulses have been used for bubble detection and tracking (Li et al., 2014). This timing constraint means that cavitation activity occurring during therapeutic ultrasound exposures (often thousands of cycles) would be missed, and with it, information about the therapy process would remain unknown. This limitation is especially important if using solid cavitation nuclei, which are essentially anechoic unless driven with a low-frequency excitation (e.g., therapy beam).

Passive Ultrasound

Passive acoustic mapping (PAM) methods are intended to detect, localize, and quantify cavitation activity based on analysis of bubble-scattered sound (for a review of the current art, see Haworth et al., 2017; Gray and Coussios, 2018). Unlike active-imaging modalities, PAM images may be computed at any time during a therapeutic ultrasound exposure and are decoupled from restrictions on timing, pulse length, or bandwidth imposed by the means of cavitation generation. Because of this timing independence, PAM methods yield fundamentally different (and arguably more relevant) information about micro-bubble activity. For example, features in the passively received spectrum such as half-integer harmonics (**Figure 1**) may be used to distinguish cavitation types from each other and from nonlinearities in the system being monitored and therefore may indicate the local therapeutic effects being applied.

The processes for PAM image formation are illustrated in **Figure 2**. Suppose a single bubble located at position x_s radiates sound within a region of interest (ROI), such as a tumor undergoing therapeutic ultrasound exposure. Under ideal conditions, the bubble-emitted field propagates spherically, where it may be detected by an array of receivers, commonly a conventional handheld diagnostic array placed on the skin. PAM methods estimate the location of the bubble based on relative delays between array elements due to the curvature of the received wave fronts. This stands in contrast to conventional active methods that localize targets using the time delay between active transmission and echo reception.

After filtering raw array data to remove unwanted signals (such as the fundamental frequency of the active ultrasound that created the cavitation), PAM algorithms essentially run a series of spatial and temporal signal similarity tests consisting of two basic steps. First, the array data are steered to a point (x) in the ROI by adding time shifts to compensate for the path length between x and each array element. If the source actually was located at the steering location ($x = x_s$), then all the array signals would be temporally aligned. Second, the steered data are combined, which in its simplest form involves summation. In more sophisticated forms, the array signal covariance matrix is scaled by weight factors optimized to reduce interference from neighboring bubbles (Coviello et al., 2015).

Regardless of the procedural details, the calculation typically yields an array-average signal power for each steering location in the ROI. This quantity is maximized when the array has been steered to the source location, and the map has its best spatial resolution when interference from other sources has been suppressed. The processing illustration in **Figure 2** is in the time

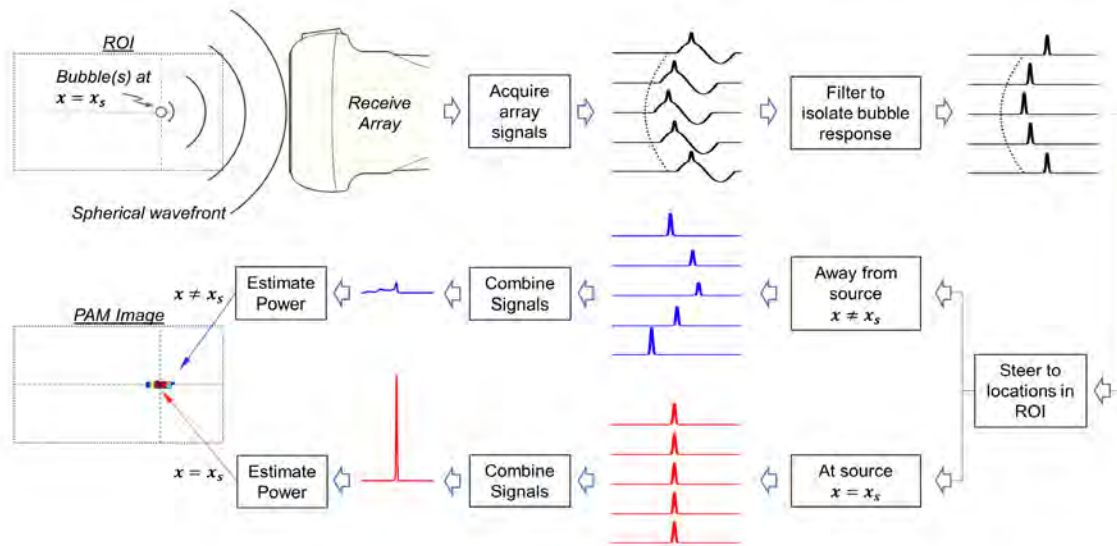


Figure 2. Time domain illustration of passive acoustic mapping (PAM) processing. Bubble emissions are received on an array of sensors. Signals (**black**) have relative delays that are characteristic of the distance between the array and the source location. After filtering the raw data to isolate either broadband or narrowband acoustic emissions of interest, the first processing step is to steer the array to a point in the region of interest (ROI) by applying time shifts to each array element. If the steered location matches that of the source ($x = x_s$), the signals will be time aligned (**red**); otherwise, the signals will be temporally misaligned (**blue**; $x \neq x_s$). The second processing step combines the time-shifted signals to estimate signal power; poorly correlated data will lead to a low power estimate while well-correlated data will identify the source. Repeating this process over a grid in the ROI leads to an image of source (bubble) strength (**bottom left**). The image has a dynamic range of 100, and **red** indicates a maximum value.

domain, but frequency domain implementations offer equivalent performance with potentially lower calculation times.

The roots of PAM techniques are found in passive beamforming research performed in the context of seismology, underwater acoustics, and radar. The utility of these techniques comes from their specific benefits when applied to noninvasive cavitation monitoring.

- Images are formed in the near field of the receive array so that sources may be identified in at least two dimensions (e.g., distance and angle).
- Received data may be filtered to identify bubble-specific emissions (half-integer harmonics or broadband noise elevation), thereby decluttering the image of nonlinear background scattering and identifying imaging regions that have different cavitation behaviors.
- A single diagnostic ultrasound array system can be used to provide both tissue imaging and cavitation mapping capabilities that are naturally coaligned so that the monitoring process can describe the tissue and bubble status before, during, and after therapy.
- Real-time PAM may allow automated control of the therapy process to ensure procedural safety.

For both passive and active ultrasonic methods, image quality and quantitative accuracy may be limited by uncertainties

in tissue sound speed and attenuation. Unlike MR or active ultrasonic methods, PAM data must be superimposed on tissue morphology images produced by other imaging methods to provide a context for treatment guidance and monitoring.

Clinical PAM Example

Over the last decade, PAM research has progressed from small-rodent to large-primate in vivo models, and recently, a clinical cavitation mapping dataset was collected during a Phase 1 trial of ultrasound-mediated liver heating for drug release from thermally sensitive liposomes (Lyon et al., 2018). **Figure 3** shows an axial computed tomography (CT) image of one trial participant, including the targeted liver tumor. The incident therapeutic-focused ultrasound beam (FUS; **Figure 3, red arrow**) was provided by a clinically approved system, while the PAM data (**Figure 3, blue arrow**) was collected using a commercially available curvilinear diagnostic array. The CT-overlaid PAM image (and movie showing six consecutive PAM frames, see acousticstoday.org/gray-media) was generated using a patient-specific sound speed estimate and an adaptive beamformer to minimize beamwidth. Although the monitoring was performed over an hour-long treatment, only a small handful of cavitation events was detected (<0.1% of exposures). This was as expected given that no exogenous microbubbles were used and the treatment settings

were intended to avoid thermally significant cavitation. This example shows the potential for real-time mapping of bubble activity in clinically relevant targets using PAM techniques.

Using Bubbles

Bubble Behaviors

The seemingly simple system of an ultrasonically driven bubble in a homogeneous liquid can exhibit a broad range of behaviors (Figure 4). In an unbounded medium, bubble wall motion induces fluid flow, sound radiation, and heating (Leighton, 1994) and may spur its own growth by rectified diffusion, a net influx of mass during ultrasonic rarefaction cycles. When a bubble grows sufficiently large during the rarefactional half cycle of the acoustic wave, it will be unable to resist the inertia of the surrounding liquid during the compressional half cycle and will collapse to a fraction of its original size. The resulting short-lived concentration of energy and mass further enhances sound radiation, heating rate, fluid flow, and particulate transport and can lead to a chemical reaction (sonochemistry) and light emission (sonoluminescence). Regarding the spatially and temporally intense action of this “inertial cavitation,” it has been duly noted that in a simple laboratory experiment “...one can create the temperature of the sun’s surface, the pressure of deep oceanic trenches, and the cooling rate of molten metal splatted onto a liquid-helium-cooled surface!” (Suslick, 1990, p. 1439).

Further complexity is introduced when the bubble vibrates near an acoustic impedance contrast boundary such as a glass slide in an *in vitro* experiment or blood vessel wall in tissue. Nonlinearly generated circulatory fluid flow known as “microstreaming” is produced as the bubble oscillates about its translating center of mass (Marmottant and Hilgenfeldt, 2003) and can both enhance transport of nearby therapeutic particles (drugs or sub-micron nuclei) and amplify fluid shear stresses that deform or rupture nearby cells (“microdeformation” in Figure 4).

Theracoustic Applications:

Furnace, Mixer, and Sniper Bubbles

Suitably nucleated, mapped, and controlled, all of the aforementioned phenomena find therapeutically beneficial applications within the human body. Here, we present a subset of the ever-expanding range of applications involving acoustic cavitation.

One of the earliest, and now most widespread, uses of therapeutic ultrasound is thermal, whereby an extracorporeal transducer is used to selectively heat and potentially destroy a well-defined tissue volume (“ablation”; Kennedy, 2005). A key challenge in selecting the optimal acoustic parameters to achieve this is the inevitable compromise between propaga-

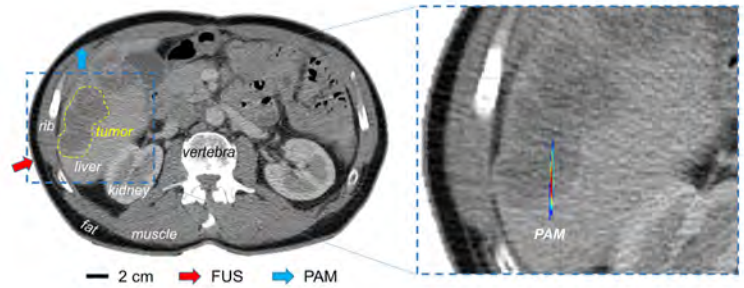


Figure 3. Example of passive cavitation mapping during a clinical therapeutic ultrasound procedure. **Left:** axial CT slice showing thoracic organs, including the tumor targeted for treatment, with red and blue arrows indicating the directions of therapeutic focused ultrasound (FUS) incidence and PAM data collection, respectively. **Right:** enlarged subregion (left, blue dashed-line box) in which a PAM image was generated. Maximum (red) and minimum (blue) color map intensities cover one order of magnitude. A video of six successive PAM frames spanning a total time period of 500 microseconds is available at (acousticstoday.org/gray-media).

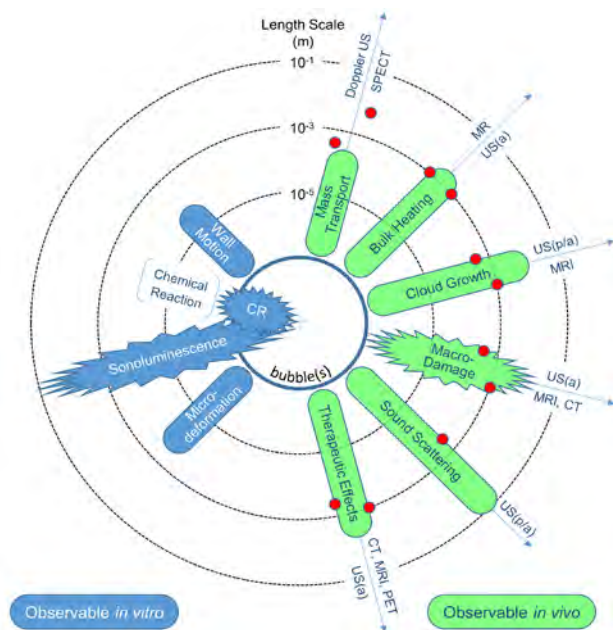


Figure 4. Illustration of bubble effects and length scales. **Green**, *in vivo* measurement feasibility; **jagged shapes** indicate reliance on inertial cavitation; **red dots**, best spatial resolution; **text around radial arrows**, demonstrated noninvasive observation methods. SPECT, single photon emission computed tomography; US, ultrasound; a, active; p, passive; MRI, magnetic resonance imaging; CT, X-ray computed tomography; PET, positron emission tomography.

tion depth, optimally achieved at lower frequencies, and the local rate of heating, which is maximized at higher frequencies. “Furnace” bubbles provide a unique way of overcoming this limitation (Holt and Roy, 2001); by redistributing part of the incident energy into broadband acoustic emissions that are more readily absorbed, inertial cavitation facilitates highly localized heating from a deeply propagating low-frequency wave (Coussios et al., 2007).

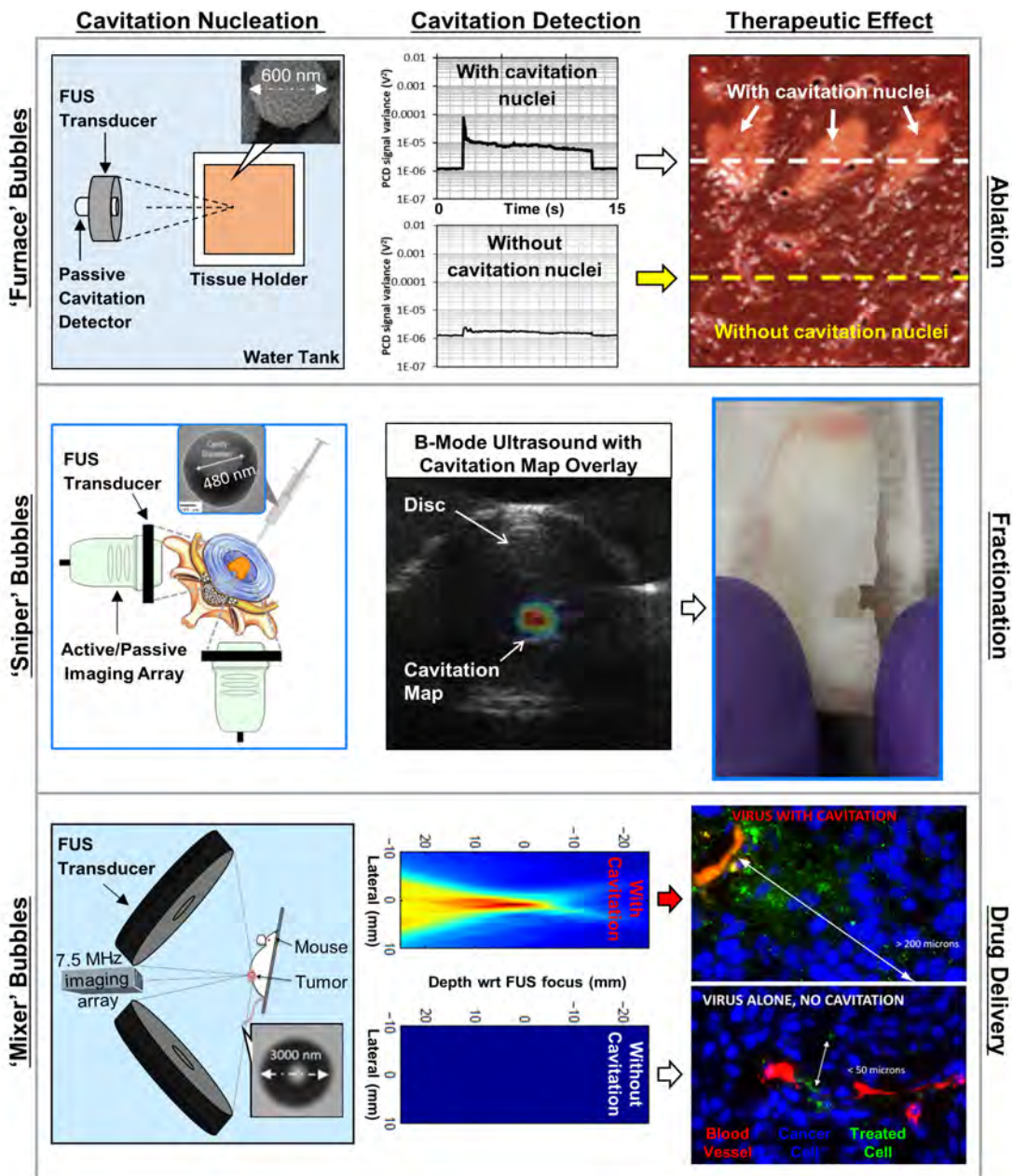


Figure 5. Nucleation and cavitation detection strategies for a range of emerging theracoustic applications. **Top row:** passively monitored cavitation-mediated thermal ablation nucleated by locally injected gas-stabilizing particles in liver tissue. **Center row:** dual-array passively mapped cavitation-mediated fractionation of the intervertebral disc, nucleated by gas-stabilizing solid polymeric particles. **Bottom row:** single-array passively mapped cavitation-enhanced drug delivery to tumors, following systemic administration of lipid-shelled microbubbles and an oncolytic virus. See text for a fuller explanation.

This process is illustrated in **Figure 5, top row**, using a sample of bovine liver exposed to FUS while monitoring the process with a single-element passive-cavitation detector (PCD). In the absence of cavitation nuclei, the PCD signal is weak and the tissue is unaltered. However, when using these same FUS settings in the presence of locally injected cavitation nuclei, the PCD signal is elevated by an order of magnitude and distinct regions of tissue ablation (in **Figure 5, top right, light pink regions** correspond to exposures at three locations) are observed (Hockham, 2013). Because the ultrasound-based

monitoring of temperature remains extremely challenging, exploiting acoustic cavitation to mediate tissue heating enables the use of passive cavitation detection and mapping as a means of both monitoring (Jensen et al., 2013) and controlling (Hockham et al., 2010) the treatment in real time.

There are several emerging biomedical applications where the use of ultrasound-mediated heating is not appropriate due to the potential for damage to adjacent structures, and tissue disruption must be achieved by mechanical means

alone. In this context, “sniper”-collapsing bubbles come to the rescue by producing fluid jets and shear stresses that kill cells or liquify extended tissue volumes (Khokhlova et al., 2015). More recent approaches, such as in **Figure 5, center row**, have utilized gas-stabilizing solid nanoparticles to promote and sustain inertial cavitation activity. In this example, a pair of FUS sources initiate cavitation in an intervertebral disc of the spinal column while a pair of conventional ultrasound arrays is used to produce conventional (“B-mode”) diagnostic and PAM images during treatment. The region of elevated cavitation activity (**Figure 5, center row, center, red dot** on the B-mode image) corresponds to sources of broadband emissions detected and localized by PAM and also identifies the location and size of destroyed tissue. Critically, this theracoustic configuration has enabled highly localized disintegration of collagenous tissue in the central part of the disc without affecting the outer part or the spinal canal, potentially enabling the development of a new minimally invasive treatment for lower back pain (Molinari, 2012).

Acoustic excitation is not always required to act as the primary means of altering biology but can also be deployed synergistically with a drug or other therapeutic agent to enhance its delivery and efficacy. In this context, “mixer” bubbles have a major role to play; by imposing shear stresses at tissue interfaces and by transferring momentum to the surrounding medium, they can both increase the permeability and convectively transport therapeutic agents across otherwise impenetrable biological interfaces.

One such barrier is presented by the vasculature feeding the brain, which, to prevent the transmission of infection, exhibits very limited permeability that hinders the delivery of drugs to the nervous system. However, noninertial cavitation may reversibly open this so-called blood-brain barrier (see article in *Acoustics Today* by Konofagou, 2017). A second such barrier is presented by the upper layer of the skin, which makes it challenging to transdermally deliver drugs and vaccines without a needle. Recent studies have indicated that the creation of a “patch” containing not only the drug or vaccine but also inertial cavitation nuclei (Kwan et al., 2015) can enable ultrasound to simultaneously permeabilize the skin and transport the therapeutic to hundreds of microns beneath the skin surface to enable needle-free immunization (Bhatnagar et al., 2016). Last but not least, perhaps the most formidable barrier to drug delivery is presented by tumors where the elevated internal pressure, sparse vascularity, and dense extracellular matrix hinder the ability of anticancer drugs to reach cells far removed from blood vessels. Sustained inertial cavita-

tion nucleated by either microbubbles (Carlisle et al., 2013) or submicron cavitation nuclei (Myers et al., 2016) has been shown to enable successful delivery of next-generation, larger anticancer therapeutics to reach each and every cell within the tumor, significantly enhancing their efficacy.

An example is shown in **Figure 5, bottom row**, where a pair of FUS sources was used for in vivo treatment of a mouse tumor using an oncolytic virus (140 nm) given intravenously. In the absence of microbubbles, the PAM image (**Figure 5, bottom row, center**) indicates no cavitation, and only the treated cells (**Figure 5, bottom row, center, green**) are those directly adjacent to the blood vessel (**Figure 5, bottom row, center, red**). However, when microbubbles were coadministered with the virus, the penetration and distribution of treatment were greatly enhanced, correlating with broadband acoustic emissions associated with inertial cavitation in the tumor. Excitingly, noninvasively mapping acoustic cavitation mediated by particles that are coadministered and similarly sized to the drug potentially makes it possible to monitor and confirm successful drug delivery to target tumors during treatment for the very first time.

Final Thoughts

Acoustic cavitation demonstrably enables therapeutic modulation of a number of otherwise inaccessible physiological barriers, including crossing the skin, delivering drugs to tumors, accessing the brain and central nervous system, and penetrating the cell. Much remains to be done, both in terms of understanding and optimizing the mechanisms by which oscillating bubbles mediate biological processes and in the development of advanced, indication-specific technologies for nucleating, promoting, imaging, and controlling cavitation activity in increasingly challenging anatomical locations. Suitably nucleated, mapped, and controlled, therapeutic cavitation enables acoustics to play a major role in shaping the future of precision medicine.

Acknowledgments

We gratefully acknowledge the continued support over 15 years from the United Kingdom Engineering and Physical Sciences Research Council (Awards EP/F011547/1, EP/L024012/1, EP/K021729/1, and EP/I021795/1) and the National Institute for Health Research (Oxford Biomedical Research Centre). Constantin-C. Coussios gratefully acknowledges support from the Acoustical Society of America under the 2002-2003 F. V. Hunt Postdoctoral Fellowship in Acoustics. Last but not least, we are hugely grateful to all the clinical and postdoctoral research fellows, graduate students, and collaborators who have

contributed to this area of research and to the broader therapeutic ultrasound and “theracoustic” cavitation community for its transformative ethos and collaborative spirit.

References

- Ainslie, M. A., and Leighton, T. G. (2011). Review of scattering and extinction cross-sections, damping factors, and resonance frequencies of a spherical gas bubble. *The Journal of the Acoustical Society of America* 130, 3184-3208. <https://doi.org/10.1121/1.3628321>.
- Arvanitis, C. D., Bazan-Peregrino, M., Rifai, B., Seymour, L. W., and Coussios, C. C. (2011). Cavitation-enhanced extravasation for drug delivery. *Ultrasound in Medicine & Biology* 37, 1838-1852. <https://doi.org/10.1016/j.ultrasmedbio.2011.08.004>.
- Atchley, A. A., and Prosperetti, A. (1989). The crevice model of bubble nucleation. *The Journal of the Acoustical Society of America* 86, 1065-1084. <https://doi.org/10.1121/1.398098>.
- Bhatnagar, S., Kwan, J. J., Shah, A. R., Coussios, C.-C., and Carlisle, R. C. (2016). Exploitation of sub-micron cavitation nuclei to enhance ultrasound-mediated transdermal transport and penetration of vaccines. *Journal of Controlled Release* 238, 22-30. <https://doi.org/10.1002/jps.23971>.
- Burgess, M., and Porter, T. (2015). On-demand cavitation from bursting droplets. *Acoustics Today* 11(4), 35-41.
- Carlisle, R., Choi, J., Bazan-Peregrino, M., Laga, R., Subr, V., Kostka, L., Ulbrich, K., Coussios, C.-C., and Seymour, L. W. (2013). Enhanced tumor uptake and penetration of virotherapy using polymer stealthing and focused ultrasound. *Journal of the National Cancer Institute* 105, 1701-1710. <https://doi.org/10.1093/jnci/djt305>.
- Coussios, C. C., Farny, C. H., ter Haar, G., and Roy, R. A. (2007). Role of acoustic cavitation in the delivery and monitoring of cancer treatment by high-intensity focused ultrasound (HIFU). *International Journal of Hyperthermia* 23, 105-120. <https://doi.org/10.1080/02656730701194131>.
- Coussios, C. C., and Roy, R. A. (2008). Applications of acoustics and cavitation to non-invasive therapy and drug delivery. *Annual Review of Fluid Mechanics* 40, 395-420. <https://doi.org/10.1146/annurev.fluid.40.111406.102116>.
- Couture, O., Hingot, V., Heiles, B., Muleki-Seya, P., and Tanter, M. (2018). Ultrasound localization microscopy and super-resolution: A state of the art. *IEEE Transactions on Ultrasonics Ferroelectrics and Frequency Control* 65, 1304-1320. <https://doi.org/10.1109/tuffc.2018.2850811>.
- Coviello, C., Kozick, R., Choi, J., Gyongy, M., Jensen, C., Smith, P., and Coussios, C. (2015). Passive acoustic mapping utilizing optimal beamforming in ultrasound therapy monitoring. *The Journal of the Acoustical Society of America* 137, 2573-2585. <https://doi.org/10.1121/1.4916694>.
- Dowling, A. P., and Ffowcs Williams, J. (1983). *Sound and Sources of Sound*. Ellis Horwood, Chichester, UK.
- Fox, F. E., and Herzfeld, K. F. (1954). Gas bubbles with organic skin as cavitation nuclei. *The Journal of the Acoustical Society of America* 26, 984-989. <https://doi.org/10.1121/1.1907466>.
- Gray, M. D., and Coussios, C. C. (2018). Broadband ultrasonic attenuation estimation and compensation with passive acoustic mapping. *IEEE Transactions on Ultrasonics Ferroelectrics and Frequency Control* 65, 1997-2011. <https://doi.org/10.1109/tuffc.2018.2866171>.
- Haworth, K. J., Bader, K. B., Rich, K. T., Holland, C. K., and Mast, T. D. (2017). Quantitative frequency-domain passive cavitation imaging. *IEEE Transactions on Ultrasonics Ferroelectrics and Frequency Control* 64, 177-191. <https://doi.org/10.1109/tuffc.2016.2620492>.
- Hockham, N. (2013). *Spatio-Temporal Control of Acoustic Cavitation During High-Intensity Focused Ultrasound Therapy*. PhD Thesis, University of Oxford, Oxford, UK.
- Hockham, N., Coussios, C. C., and Arora, M. (2010). A real-time controller for sustaining thermally relevant acoustic cavitation during ultrasound therapy. *IEEE Transactions on Ultrasonics Ferroelectrics and Frequency Control* 57, 2685-2694. <https://doi.org/10.1109/tuffc.2010.1742>.
- Holt, R. G., and Roy, R. A. (2001). Measurements of bubble-enhanced heating from focused, MHz-frequency ultrasound in a tissue-mimicking material. *Ultrasound in Medicine and Biology* 27, 1399-1412.
- Jensen, C., Cleveland, R., and Coussios, C. (2013). Real-time temperature estimation and monitoring of HIFU ablation through a combined modeling and passive acoustic mapping approach. *Physics in Medicine and Biology* 58, 5833. <https://doi.org/10.1088/0031-9155/58/17/5833>.
- Kennedy, J. E. (2005). High-intensity focused ultrasound in the treatment of solid tumours. *Nature Reviews Cancer* 5, 321-327. <https://doi.org/10.1038/nrc1591>.
- Khokhlova, V. A., Fowlkes, J. B., Roberts, W. W., Schade, G. R., Xu, Z., Khokhlova, T. D., Hall, T. L., Maxwell, A. D., Wang, Y. N., and Cain, C. A. (2015). Histotripsy methods in mechanical disintegration of tissue: towards clinical applications. *International Journal of Hyperthermia* 31, 145-162. <https://doi.org/10.3109/02656736.2015.1007538>.
- Konofagou, E. E. (2017). Trespassing the barrier of the brain with ultrasound. *Acoustics Today* 13(4), 21-26.
- Kwan, J. J., Graham, S., Myers, R., Carlisle, R., Stride, E., and Coussios, C. C. (2015). Ultrasound-induced inertial cavitation from gas-stabilizing nanoparticles. *Physical Review E* 92, 5. <https://doi.org/10.1103/PhysRevE.92.023019>.
- Leighton, T. G. (1994). *The Acoustic Bubble*. Academic Press, London, UK.
- Li, T., Khokhlova, T. D., Sapozhnikov, O. A., O'Donnell, M., and Hwang, J. H. (2014). A new active cavitation mapping technique for pulsed HIFU applications-bubble doppler. *IEEE Transactions on Ultrasonics Ferroelectrics and Frequency Control* 61, 1698-1708. <https://doi.org/10.1109/tuffc.2014.006502>.
- Lyon, P. C., Gray, M. D., Mannaris, C., Folkes, L. K., Stratford, M., Campo, L., Chung, D. Y. F., Scott, S., Anderson, M., Goldin, R., Carlisle, R., Wu, F., Middleton, M. R., Gleeson, F. V., and Coussios, C. C. (2018). Safety and feasibility of ultrasound-triggered targeted drug delivery of doxorubicin from thermosensitive liposomes in liver tumours (TARDOX): A single-centre, open-label, phase 1 trial. *The Lancet Oncology* 19, 1027-1039.
- Marmottant, P., and Hilgenfeldt, S. (2003). Controlled vesicle deformation and lysis by single oscillating bubbles. *Nature* 423, 153-156. <https://doi.org/10.1038/nature01613>.
- Matula, T. J., and Chen, H. (2013). Microbubbles as ultrasound contrast agents. *Acoustics Today* 9(1), 14-20.
- Molinari, M. (2012). *Mechanical Fractionation of the Intervertebral Disc*. PhD Thesis, University of Oxford, Oxford, UK.
- Myers, R., Coviello, C., Erbs, P., Follope, J., Rowe, C., Kwan, J., Crake, C., Finn, S., Jackson, E., Balloul, J.-M., Story, C., Coussios, C., and Carlisle, R. (2016). Polymeric cups for cavitation-mediated delivery of oncolytic vaccinia virus. *Molecular Therapy* 24, 1627-1633. <https://doi.org/10.1038/mt.2016.139>.
- Rapoport, N., Gao, Z. G., and Kennedy, A. (2007). Multifunctional nanoparticles for combining ultrasonic tumor imaging and targeted chemotherapy. *Journal of the National Cancer Institute* 99, 1095-1106. <https://doi.org/10.1093/jnci/djm043>.
- Rieke, V., and Pauly, K. (2008). MR thermometry. *Journal of Magnetic Resonance Imaging* 27, 376-390. <https://doi.org/10.1002/jmri.21265>.
- Stride, E. P., and Coussios, C. C. (2010). Cavitation and contrast: The use of bubbles in ultrasound imaging and therapy. *Proceedings of the Institution of Mechanical Engineers, Part H: Journal of Engineering in Medicine* 224, 171-191. <https://doi.org/10.1243/09544119jeim622>.
- Suslick, K. S. (1990). Sonochemistry. *Science* 247, 1439-1445. <https://doi.org/10.1126/science.247.4949.1439>.
- ter Haar, G., and Coussios, C. (2007). High intensity focused ultrasound: physical principles and devices. *International Journal of Hyperthermia* 23, 89-104. <https://doi.org/10.1080/02656730601186138>.



Michael D. Gray is a senior research fellow at the Biomedical Ultrasonics, Biotherapy and Biopharmaceuticals Laboratory (BUBBL), Institute of Biomedical Engineering, University of Oxford, Oxford, UK. His research interests include the use of sound, magnetism, and light

for targeted drug delivery; clinical translation of cavitation monitoring techniques; and hearing in marine animals. He holds a PhD from the Georgia Institute of Technology (2015) and has over 26 years of experience in acoustics applications ranging from cells to submarines.



Eleanor Stride is a professor of biomaterials at the University of Oxford, Oxford, UK, specializing in stimuli responsive drug delivery. She obtained her BEng and PhD in mechanical engineering from University College London, UK, before moving to Oxford in 2011. She

has published over 150 academic papers, has 7 patents, and is a director of 2 spinout companies set up to translate her research into clinical practice. Her contributions have been recognized with several awards, including the 2015 Acoustical Society of America (ASA) Bruce Lindsay Award and the Institution of Engineering and Technology (IET) A. F. Harvey Prize. She became a fellow of the Royal Academy of Engineering in 2017 and of the ASA in 2018.



Constantin-C. Coussios is the director of the Institute of Biomedical Engineering and the holder of the first statutory chair in Biomedical Engineering at the University of Oxford, Oxford, UK, where he founded and heads the Biomedical Ultrasonics, Biotherapy and Biopharmaceuticals Laboratory (BUB-

BL) since 2004. He is a recipient of the Acoustical Society of America (ASA) F. V. Hunt Postdoctoral Fellowship (2002), the ASA Bruce Lindsay Award in 2012, and the Silver Medal from the UK Royal Academy of Engineering in 2017 and has been a fellow of the ASA since 2009. He holds BA, MEng, and PhD (2002) degrees from the University of Cambridge, Cambridge, UK and has cofounded two medical device companies that exploit acoustic cavitation for minimally invasive surgery (OrthoSon Ltd.) and oncological drug delivery (Ox-Sonics Ltd.).

NGC[®] TESTING SERVICES

ACOUSTICAL • FIRE • STRUCTURAL • ANALYTICAL™

Over 50 Years of Test Services

NVLAP Accredited (Code 200291-0)

IAS Accredited (Lab Code 216)

ISO/IEC 17025 Compliant

Test Capabilities Include:

E492 IIC, E2179 Delta IIC E90 STC

C423 NRC, E1414 CAC, E1111 AC

Sound Power, Pipe Lagging, SAE J1400

E84 Flame Spread, E119 Fire Endurance

NGC Testing Services • 1650 Military Road

Buffalo, NY 14217 • Tel: 716-873-9750

ngctestingservices.com

ASA SCHOOL 2020

Living in the Acoustic Environment

May 9-10, 2020 • Itasca, IL

- **Two-Day Program** Lectures, demonstrations, and discussions by distinguished acousticians covering interdisciplinary topics in eight technical areas
- **Participants** Graduate students and early career acousticians in all areas of acoustics
- **Location** Eaglewood Resort and Spa, Itasca, IL
- **Dates** May 9-10, 2020, immediately preceding the ASA spring meeting in Chicago
- **Cost** \$50 registration fee, which includes hotel, meals, and transportation from Eaglewood to the ASA meeting location
- **More Information** Application form, preliminary program, and more details will be available in November, 2019 at AcousticalSociety.org

